Science of the Total Environment 751 (2021) 141681

Contents lists available at ScienceDirect

Science of the Total Environment

journal homepage: www.elsevier.com/locate/scitotenv

Atmospheric reactive mercury concentrations in coastal Australia and the Southern Ocean

Matthieu B. Miller [a,*], Dean A. Howard [b], Ashley M. Pierce [a], Kellie R. Cook [a], Melita Keywood [c], Jennifer Powell [c], Mae S. Gustin [d], Grant C. Edwards [a,1]

[a] Department of Environmental Sciences, Faculty of Science and Engineering, Macquarie University, Sydney, NSW 2113, Australia
[b] Institute of Arctic and Alpine Research, University of Colorado Boulder, Boulder, CO 80303, United States
[c] Centre for Australian Climate and Weather Research, Australian Commonwealth Scientific and Industrial Research Organization, Melbourne, VIC, Australia
[d] Department of Natural Resources and Environmental Sciences, University of Nevada, Reno, NV 89557, United States

HIGHLIGHTS

- Atmospheric Hg was measured at 2 sites in Australia and over the Southern Ocean.
- GEM was measured using a Tekran 2537 and RM with cation exchange membranes.
- Seasonal variations in RM concentration were slight or negligible.
- RM concentrations in the MBL were higher than reported in previous studies.
- This has important implications for globally coupled ocean-atmosphere models.

GRAPHICAL ABSTRACT

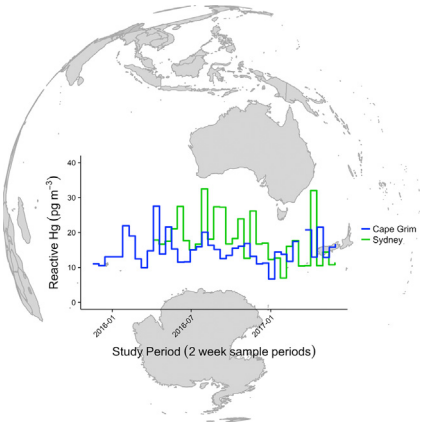

ARTICLE INFO

Article history:
Received 1 May 2020
Received in revised form 11 August 2020
Accepted 11 August 2020
Available online 12 August 2020

Editor: Xinbin Feng

Keywords:
Gaseous elemental mercury
Gaseous oxidized mercury
Tekran 2537
Cape Grim Baseline Air Pollution Station
Southern hemisphere
Cation exchange membranes

ABSTRACT

Mercury (Hg), especially reactive Hg (RM), data from the Southern Hemisphere (SH) are limited. In this study, long-term measurements of both gaseous elemental Hg (GEM) and RM were made at two ground-based monitoring locations in Australia, the Cape Grim Baseline Air Pollution Station (CGBAPS) in Tasmania, and the Macquarie University Automatic Weather Station (MQAWS) in Sydney, New South Wales. Measurements were also made on board the Australian RV Investigator (RVI) during an ocean research voyage to the East Antarctic coast. GEM was measured using the standard Tekran® 2537 series analytical platform, and RM was measured using cation exchange membranes (CEM) in a filter-based sampling method. Overall mean RM concentrations at CGBAPS and MQAWS were 15.9 ± 6.7 pg m^{-3} and 17.8 ± 6.6 pg m^{-3}, respectively. For the 10-week austral summer period on RVI, mean RM was 23.5 ± 6.7 pg m^{-3}.

RM concentrations at CGBAPS were seasonally invariable, while those at MQAWS were significantly different between summer and winter due to seasonal changes in synoptic wind patterns. During the RVI voyage, RM concentrations were relatively enhanced along the Antarctic coast (up to 30 pg m^{-3}) and GEM concentrations were variable (0.2 to 0.9 ng m^{-3}), suggesting periods of enrichment and depletion. Both RM and GEM concentrations were relatively lower while transiting the Southern Ocean farther north of Antarctica. RM concentrations measured in this study were higher in comparison to most other reported measurements of RM in the global

* Corresponding author.
E-mail address: matthieu.b.miller@gmail.com (M.B. Miller).
[1]Deceased 10 September 2018.

https://doi.org/10.1016/j.scitotenv.2020.141681

marine boundary layer (MBL), especially for remote SH locations. As observations of GEM and RM concentrations inform global ocean-atmosphere model simulations of the atmospheric Hg budget, our results have important implications for understanding of total atmospheric Hg (TAM).

1. Introduction

Mercury (Hg) is a pervasive environmental toxin with global distribution via a significant atmospheric cycle that includes emission, deposition, and re-emission. Elemental Hg, a unique semi-volatile liquid metal, is readily emitted to the atmosphere in the gas phase where it is transported widely and subject to a number of physiochemical processes. These processes cause total atmospheric Hg (TAM) to fluctuate, usually to a small degree but sometimes radically, between several broad forms that defy easy practical differentiation: gaseous elemental mercury (GEM), gaseous oxidized mercury (GOM), and particulate bound mercury (PBM). GEM is usually thought to comprise the bulk of TAM (>95%), though it is known to convert almost entirely to GOM or PBM under certain oxidative conditions (Ebinghaus et al., 2002; Obrist et al., 2011; Schroeder et al., 1998; Steffen et al., 2002; Temme et al., 2003). Where GOM and PBM are not readily distinguishable with certainty, they can be quantified together as reactive mercury (RM), also referred to as Hg(II) or Hg^{2+} (Weiss-Penzias et al., 2015).

The calibrated measurement of trace concentrations of GEM is technically achievable to high precision (±3% uncertainty) using preconcentration and cold vapor atomic fluorescence spectrometry (CVAFS). The principal analytical instrument is the Tekran® 2537 A/B/X Automated Ambient Air Analyzer. Measurement of GEM is routine in many atmospheric monitoring networks to a nominal level of standardization (UNEP, 2016). However, practically achievable instrument uncertainty may average around 10%, with some inter-instrument biases as high as 20% (Gustin and Jaffe, 2010; Slemr et al., 2015). There is an open question as to whether the 2537 measures GEM or TGM. Part of this question is due to the likelihood that many sample inlet configurations preclude a true TGM measurement, but may still allow some Hg^{2+} to pass through, resulting in an ambiguous value between GEM and TGM (Steffen et al., 2008; Steffen et al., 2002).

The measurement of RM is comparatively less straight forward and currently depends on isolating GOM and PBM, separately or together, from a typically much larger GEM signal. Recent experimental studies have met with some success using filter methods (cf. Gustin et al., 2019; Luippold et al., 2020a, 2020b). The principle commercially available apparatus is the Tekran® 1130/1135 Hg speciation system that uses a denuder and particulate filter (0.1 μm pore size) to separate GOM and PBM, respectively, from total gaseous Hg (Landis et al., 2002). The variable levels of success in measuring atmospheric RM have been detailed in recent critical reviews (Cheng and Zhang, 2017; Gustin et al., 2015; Jaffe et al., 2014; Zhang et al., 2017). In particular, the potassium chloride (KCl) coated denuder used in the Tekran® 1130 system for GOM collection has been shown to suffer interferences from ozone and water vapor, resulting in systematic under quantification (Ambrose et al., 2013; Lyman et al., 2010; McClure et al., 2014). Also, as the system is operated with a cyclone inlet with a 2.5 μm particle size cut-point, some fraction of PBM is necessarily excluded by design.

An alternative method that has been used with some success to selectively measure RM concentrations in ambient air is a cation exchange membrane (CEM) filter system (Gustin et al., 2016; Huang and Gustin, 2015; Huang et al., 2017; Huang et al., 2013; Marusczak et al., 2017; Pierce and Gustin, 2017). The CEM filters are inert to GEM uptake (Miller et al., 2019) and have good selectivity for RM compounds (Huang et al., 2013; Lyman et al., 2016). The CEM based sampling systems typically deploy triplicate, paired CEM filters at a controlled flow rate. Each pair of filters constitutes one sample, the first filter serving as the primary collection surface, and the second filter capturing potential breakthrough. Filters are deployed for one to two weeks in order to collect a detectable quantity of RM for analysis. The long sample time, limited number of samples, and involved analytical procedure are the major drawbacks to this method.

Despite the limitations inherent to current Hg measurement techniques, the best practicable monitoring of atmospheric Hg is still required to inform environmental and human health policy. Such monitoring is extensive in the Northern Hemisphere with dozens of active sites, but only 4 to 6 non-Antarctic sites operate in the Southern Hemisphere at any one time (Sprovieri et al., 2016; UNEP, 2016). Most SH sites have only been operated continuously within the last several years, and the overall lack of long-term atmospheric Hg data in the SH, especially for reactive Hg species, constitutes a significant knowledge gap. Closing this gap will contribute to ongoing science and policy needs as expressed in the United Nations Environment Minamata Convention on Mercury (UNEP, 2013).

In this study, we report the first continuous measurements of atmospheric RM in Australia, using the CEM filter-based method. RM measurements were made in conjunction with the existing GEM monitoring program at the Cape Grim Baseline Air Pollution Station (CGBAPS) in Tasmania, and at a new site established at the Macquarie University Automatic Weather Station (MQAWS) in suburban Sydney, New South Wales. In addition, RM concentration data is presented from CEM filters deployed on the Australian Research Vessel Investigator (RVI) for the austral summer 2017 voyage in the Southern Ocean, with concurrent GEM measurements.

2. Methods

2.1. Field sites

Atmospheric Hg was measured at two temperate coastal mid-latitude sites in Australia, and on an ocean research voyage transiting the Southern Ocean from southern Australian waters to the East Antarctic coast (Fig. 1).

Cape Grim Baseline Air Pollution Station (CGBAPS) is located on the north western point of Tasmania, Australia (−40.683 S 144.690 E, 94 m a.s.l.). The site is coastal with a cool temperate oceanic climate. CGBAPS is jointly administered by the Australian Bureau of Meteorology (BoM) and the Commonwealth Scientific and Industrial Research Organization (CSIRO), and is part of the World Meteorological Organization Global Atmosphere Watch (WMO-GAW) program. The site has operated a Tekran® 2537B Ambient Air Mercury Analyzer since September 2011, and a newer Tekran® 2537× unit since June 2017.

Macquarie University Automatic Weather Station (MQAWS) is located in the northern suburbs of Sydney, New South Wales, Australia (−33.765 S 151.117 E, 67 m a.s.l.) on part of the campus sport fields, and has previously been used as an “urban background” measurement site as there are no major industrial point sources within 5 km (Mohiuddin et al., 2014). The immediate environment is an open grassy field with denser woodland areas of Lane Cove National Park just to the east, but the site is entirely surrounded by built up urban areas with a major motorway 400 m to the southwest. Though nominally inland at 16 km from the pelagic Pacific coast, the site is within the natural Sydney harbor topographical basin and can be considered a near coastal environment with a humid subtropical climate. A Tekran® 2537A has been operated intermittently at the site since May 2016.

The RV Investigator (RVI) is a 94 m state-of-the-art multidisciplinary blue water research vessel operated by CSIRO as part of the Australian

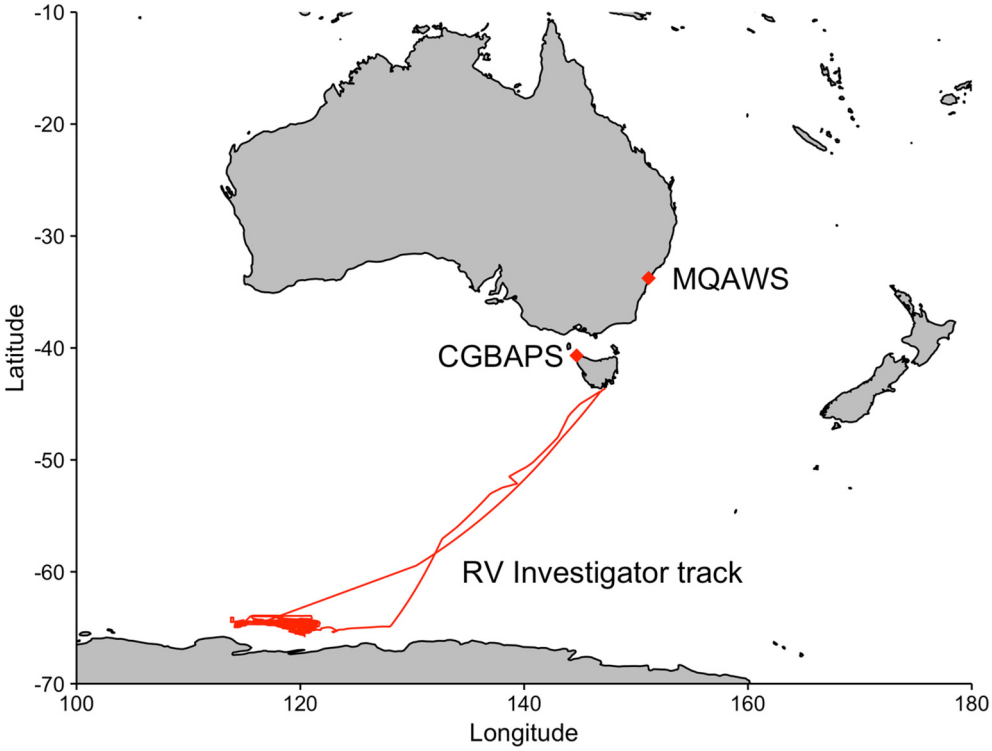

Fig. 1. Location map of ambient RM measurement sites in Australia and track of RV Investigator (RVI) research voyage in the Southern Ocean.

Marine National Facility. Voyage 1 of 2017 (January 13 – March 6) transited the Southern Ocean to the sea-ice region off the East Antarctic coast, departing and returning from the southern port of Hobart, Tasmania. The primary scientific mission was a survey of the continental shelf in the area offshore from the Totten Glacier. Aerosol sampling in the northern Antarctic atmosphere was an additional mission, and as part of the atmospheric sampling suite a Tekran® 2537A was operated in conjunction with CEM filter deployments over the duration of the voyage. Ship exhaust has not been shown to effect on-board atmospheric Hg measurements (Soerensen et al., 2010; Sommar et al., 2010).

2.2. Measurements

Gaseous elemental Hg was measured using a Tekran® 2537A ambient mercury analyzer at MQAWS, and a Tekran® 2537B unit at CGBAPS. The Hg analyzers were operated at a 5 min (min) sample frequency and 1.0 Lpm flow rate. Sample air was pulled through PTFE Teflon tubing (0.625 cm O.D.) at station top roof rail height (~4 m a.g.l.), within a conical PTFE rain shield, and an up-front fine particulate filter. At CGBAPS, the sample line was maintained at 50 °C from roof to analyzer within an opaque heating jacket. The sample inlet ports on the 2537 units were fitted with 0.2 μm PTFE particulate filters in 47 mm PFA filter assemblies. Soda lime traps (Tekran® p/n 90-13310-06) were placed in-line immediately upstream of the filter assembly to scrub acid and organic aerosols. The attached fine particulate filter and soda lime trap precludes determination of TGM on the 2537 analyzer, and so all Tekran® data is reported as GEM (Steffen et al., 2008; Steffen et al., 2002).

At CGBAPS, quality assurance and quality control followed GMOS protocols (Sprovieri et al., 2016). The 2537B analyzer was calibrated from an internal Hg vapor permeation source every 25 h, and a standard addition of Hg vapor was permeated into the sample stream following calibrations to verify Hg recovery efficiency in ambient air. The internal 2537B permeation source was verified via manual injections from a primary Hg vapor source (Tekran® 2505) twice annually. The 5 min GEM data from the 2537 units was averaged to match the 2-week sample periods corresponding to RM filter deployments. Averaging periods for which less than 50% of data was available were excluded from the final data analysis. Hourly averages of GEM were calculated over the course of the RVI track, and any hour with less than 50% data availability was excluded.

Ambient RM concentrations were measured using an adaptation of the University of Nevada Reno Reactive Mercury Active System (Gustin et al., 2016; Huang et al., 2017). The RM sampling system consists of 3 sample lines pulling ambient air at a sample flow of 1.0 Lpm, each controlled by a ball valve, with vacuum supplied by a pump (AirCadet®). Each sample line was attached to a 2-stage 47 mm PFA filter holder (Savillex®). Filter assemblies were suspended at the end of each sample line within a standardized, anodized aluminum weather shield for long term deployments. In the 2-stage filter deployment, the first upstream "A" filter serves as the primary collection filter, and the secondary downstream "B" filter captures breakthrough. The secondary filter was used to assess how efficiently the primary filter was working, and whether any problems existed, such as a filter tear or otherwise poor seal.

Cation exchange membrane (CEM) filters were deployed on each line. The CEM filter consists of a negatively charged polyethersulfone coated matrix (0.8 um pore size, Mustang® S, Pall). The CEM material has been shown to have negligible uptake of GEM (Miller et al., 2019), and good selectivity for GOM compounds (Huang and Gustin, 2015; Huang et al., 2013). Sample flow on each line was measured and adjusted at the beginning of each 2-week sample deployment and was again measured immediately preceding filter collection. The average of the beginning and ending sample flows was taken as the flow rate for calculating total sample volume. Damaged or mis-deployed filters (as noted by site operators) were excluded from the dataset, as was any filter pair with higher Hg loading on the secondary filter, always indicative of a poor filter seal or tear.

2.3. Analysis of CEM filters

At the end of each deployment, filters were collected into sterile 50 mL polypropylene sample vials using trace clean protocols. A "blank" unused filter of each type was collected with every

deployment, and these blank values were subtracted from the measured sample values. The mean blank Hg mass on CEM filters was 60 ± 44 pg at CGBAPS (n = 40), and the minimum detection limit (MDL) for a 2-week sample period (mean sample volume 20.2 m^3) was therefore 5 pg m^{-3}. At MQAWS, the mean CEM blank Hg mass was 47 ± 26 pg (n = 31) giving a 2-week MDL of 4 pg m^{-3}. The blank Hg values and MDLs are significantly less than reported in previous studies using the CEM filter technique (Gustin et al., 2016; Huang et al., 2017), and this is attributed to the use of new 50 mL vials for each sample filter versus washing and re-using glass collection vials.

CEM filters were analyzed on a Tekran® 2600 system. Analysis began with an aqueous digestion in a strongly acidic, strongly oxidizing bromine monochloride solution to liberate captured RM from the filter material and bring it into solution within the 50 mL collection vial. Digestion was followed by reduction of the aqueous Hg^{2+} to Hg^0, which was then purged from solution in an ultra-high purity argon gas flow and pre-concentrated onto gold traps. Finally, the concentrated Hg^0 was thermally desorbed from the gold traps and measured via CVAFS (EPA Method 1631, Rev. E modified, Appendix A). The total Hg measured on each pair of sample CEM filters was divided by the calculated sample volume to arrive at a 2-week integrated RM concentration. Each 2-week sample period is reported as the mean ± standard deviation of the three sample CEM filters.

Seasons were defined according to convention as Summer (Dec-Jan-Feb), Autumn (March-April-May), Winter (June-July-Aug), and Spring (Sep-Oct-Nov). Meteorological data was retrieved from CGBAPS in hourly averages and from MQAWS in 15 min averages. MQAWS precipitation data was limited and total daily precipitation from a nearby BoM weather station was substituted (Site #066156, 33.78 S 151.11 E). All meteorological data was binned into 2-week intervals corresponding to filter deployments. Wind velocity was assessed seasonally and for each 2-week sample period. In addition, wind velocity at CGBAPS was assigned to a baseline sector (bearing 190–280°) based on established station criteria, and the percentage of baseline air in each 2-week sample period was determined. Another measurement available at CGBAPS were atmospheric particle counts, determined with an Ultrafine Condensation Particle Counter (UCPC, TSI™ Model 3776) sensitive to particle sizes down to 2.5 nm. The UCPC sample inlet was at 10 m a.g.l., with a 10 μm particle size cut-point cyclone inlet. Hourly average particle counts (particles cm^{-3}) were multiplied by the hourly sample volume through the CEM filters (0.06 m^3) to arrive at number of particles per hour in the sample flow, and these hourly values were summed over each 2-week filter deployment, providing an approximation of 2-week particle loading on the filters.

For select periods of interest, air mass back trajectories were calculated using the NOAA Hybrid Particle Lagrangian Integrated Trajectory (HYSPLIT) model (Draxler and Hess, 1998). Global Data Assimilation System (GDAS) 0.5° meteorological re-analysis data was used for initiating 120 h back trajectory calculations every hour, from a single point at height equal to 0.5× the mixed layer depth. Any trajectory that bottomed-out at 0 m elevation before reaching the station was removed from analysis.

Anthropogenic point-source Hg emission data was acquired for the 2016/2017 reporting year from the Australian National Pollutant Inventory (NPI, 2017). All point sources less than 100 g yr^{-1} were rounded to 0.1 kg in figures. The occurrence of fire hotspots from biomass burning was identified using thermal anomaly data generated by the Moderate Resolution Imaging Spectroradiometer (MODIS) sensors on NASA's Terra and Aqua satellites. MODIS data (Collection 6, version 6.1, MCD14ML definitive geolocation data set) were retrieved from the NASA Fire Information for Resource Management System (FIRMS) Fire Archive. The location and intensity of bushfire activity was assessed via the Fire Radiative Power (FRP, Watts) data output. All data was processed, and figures generated in Microsoft Excel (version 16.22) and RStudio® (version 3.2.2).

3. Results

3.1. Overall long-term observations between ground-based monitoring sites

Ambient RM was measured from November 2015 through May 2017 at CGBAPS, and from April 2016 through May 2017 at MQAWS. The overall mean RM concentration was 15.9 ± 6.7 pg m^{-3} at CGBAPS (median = 14.8, range 6.7 to 48.6 pg m^{-3}, n = 39), and 17.8 ± 6.6 pg m^{-3} at MQAWS (median = 16.8, range 7.0 to 32.5 pg m^{-3}, n = 31). Comparing equivalent overlapping sample periods at both sites (April 2016 – May 2017), there was not a statistically significant difference in either mean or median RM concentrations (Welch *t*-test, $p = .4063$, Kruskall-Wallis test $p = .4657$). This was a surprising result given the relatively large differences between the sites (i.e. remote undeveloped coast versus major urban area). A frequency distribution of RM concentration by season reveals that a greater percentage of sample periods at MQAWS were at the high range of observations above 25 pg m^{-3} (Fig. 2), and it seems likely that over a longer period of observation RM concentrations at MQAWS might be significantly higher than at CGBAPS.

During the same periods, overall mean GEM concentration was 0.90 ± 0.35 ng m^{-3} (n = 146,273 5 min samples) at CGBAPS (Fig. 3a), and 0.65 ± 0.24 ng m^{-3} (n = 32,251 5 min samples) at MQAWS (Fig. 5a). A detailed discussion of seasonal trends and baseline GEM concentration at CGBAPS for the time period January 2014 to April 2017 is discussed by Howard (2018). Technical issues with the 2537 analyzer at MQAWS resulted in less than 50% data availability for many periods, precluding analysis of a complete seasonal dataset and preventing a definite assessment of GEM concentrations at MQAWS.

3.2. Reactive mercury at Cape Grim Baseline Air Pollution Station

The median temperature at CGBAPS was 13.6 °C (range 3.5 to 25.8 °C), and the median RH was 78.6% (range 41 to 100%). Total rainfall in 2016 was exceptional at 1124.2 mm (annual median total 734.6 mm). Wind direction was from the west-southwest (195 to 315°) for the majority of time in all seasons (SI Fig. 1). Wind direction was in the baseline sector (190 to 280°) 25% of the time overall, and more so in the winter (34%) and spring (33%) seasons. Wind direction was less consistent in the summer and fall, and the proportion of wind in the baseline sector was less (21% summer, 23% fall). The summer and fall periods also experienced a greater proportion of wind from the eastern sector, which can be expected to have a greater influence from terrestrial and anthropogenic sources (discussed below).

Seasonally, the highest mean RM concentration at CGBAPS was observed in the fall (16 ± 4 pg m^{-3}), including the two highest individual 2-week RM concentrations of 28 and 49 pg m^{-3} (Fig. 3c) and four of the highest five RM concentrations (Fig. 3b). These higher fall season RM concentrations correspond to a greater occurrence of non-baseline wind events from the east. However, overall seasonal mean RM concentrations (14 pg m^{-3} in the summer and winter, 13 pg m^{-3} in the spring) were not statistically significantly different (Welch *t*-test, $p > .05$), and the occurrence of above-average RM concentration periods in the fall seems to be driven by a greater prevalence of individual events rather than a systematic seasonal increase (see Section 3.3).

No relationship was apparent between RM concentration and the percent of air arriving from the CGBAPS baseline sector (Fig. 3d). This is likely a function of the long 2-week sample period for RM, during which source air can obviously be quite variable. Considering the location on a relatively narrow island promontory, it is also likely that in terms of RM the site is dominated by baseline maritime air concentrations even when this air passes over non-baseline surfaces, except for exceptional point-source events (see Section 3.3). However, the 3 sample periods with the highest proportion of baseline air (>40%) did have a lower mean RM concentration of 13 ± 2 pg m^{-3}, and this may be

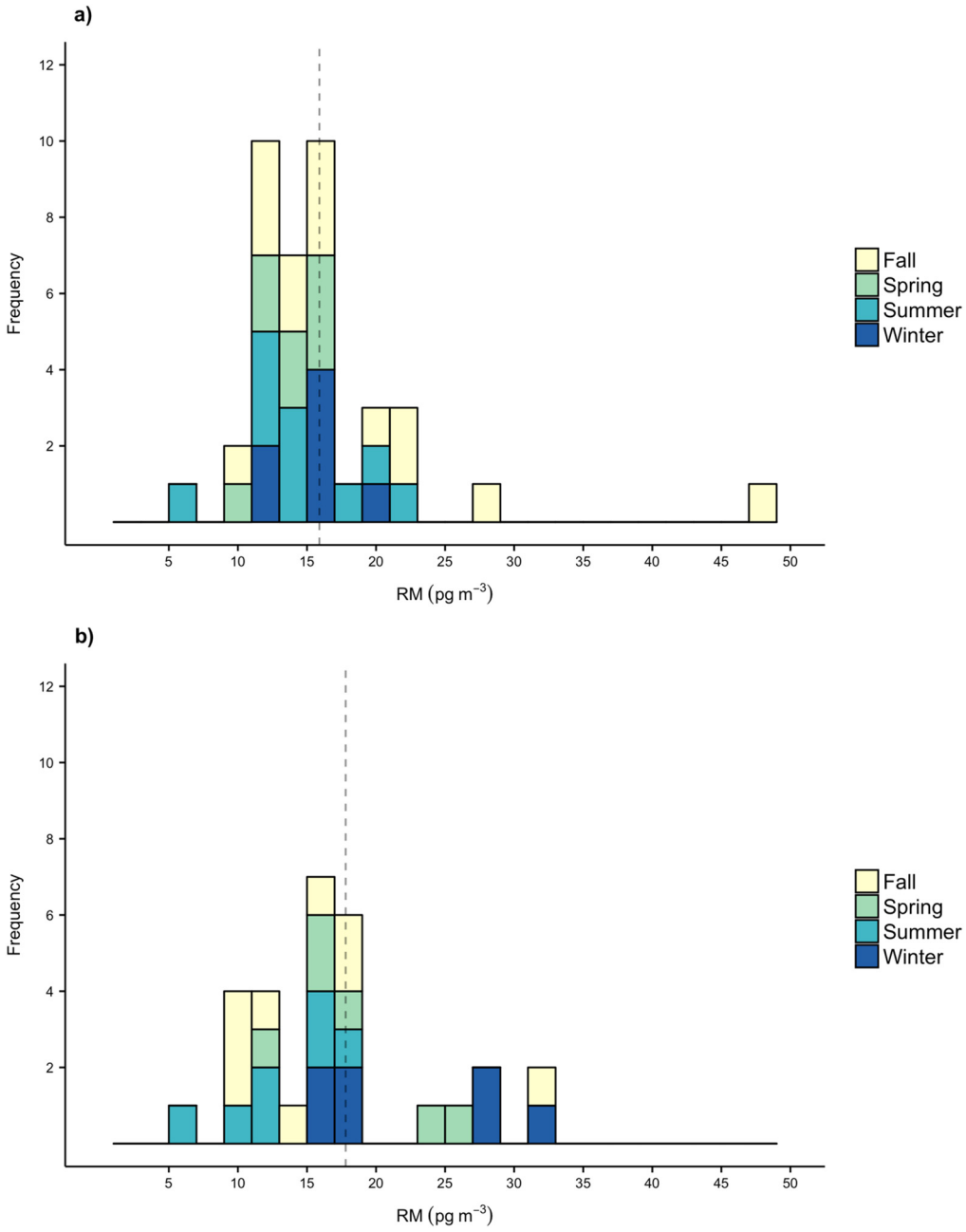

Fig. 2. Frequency distribution of observed RM concentrations at a) CGBAPS (n = 39) and b) MQAWS (n = 31). Vertical dashed lines represent overall mean RM concentrations of 15.9 ± 6.7 and 17.8 ± 6.6 pg m^{-3}, respectively.

more representative of background mid-latitude maritime RM concentrations.

Mean 2-week RM concentrations were also compared to mean 2-week values of GEM, and to median values of temperature, RH, barometric pressure, wind speed, and total 2-week precipitation (SI Fig. 2). No relationship between RM concentration and these other variables was discernible at the 2-week temporal resolution (r^2 values <0.1).

3.3. Exceptional events at Cape Grim: biomass burning and non-baseline sector

A period of widespread bushfire activity occurred in Tasmania during January – March of 2016 (SI Fig. 3). Four 2-week sample deployments in this time period measured elevated GEM concentrations (Fig. 3a). Significant plume events impacted the CGBAPS site on the night of Jan. 25–26 with peak GEM of 7.8 ng m^{-3} at 04:25, and on February 12 with peak GEM of 3.8 ng m^{-3} at 05:35 (Howard, 2018). These events were apparent in the 2-week average GEM, but the impact on RM concentration was less clear. The period Jan. 25 – Feb. 9 had an overall mean GEM concentration of 1.0 ± 0.6 ng m^{-3} and a slightly elevated RM concentration of 19 ± 1 pg m^{-3}. The following period Feb. 9–23 had a similar GEM concentration of 1.0 ± 0.4 ng m^{-3} but a relatively low RM concentration of 13 ± 1 pg m^{-3}.

Biomass combustion has been demonstrated to release primarily GEM and possibly Hg(p) (Finley et al., 2009; Howard et al., 2019; Miller et al., 2015; Weiss-Penzias et al., 2007). The fire plume events observed at CGBAPS were generated proximal to the station (within several hours trajectory travel time) and contained a high proportion of primary combustion products as evidenced by high CO/CO_2 ratios (Howard, 2018). As GOM is not a primary combustion product and the primary formation and size of PBM is uncertain, it seems likely that plume arrival times were not sufficiently long to allow secondary

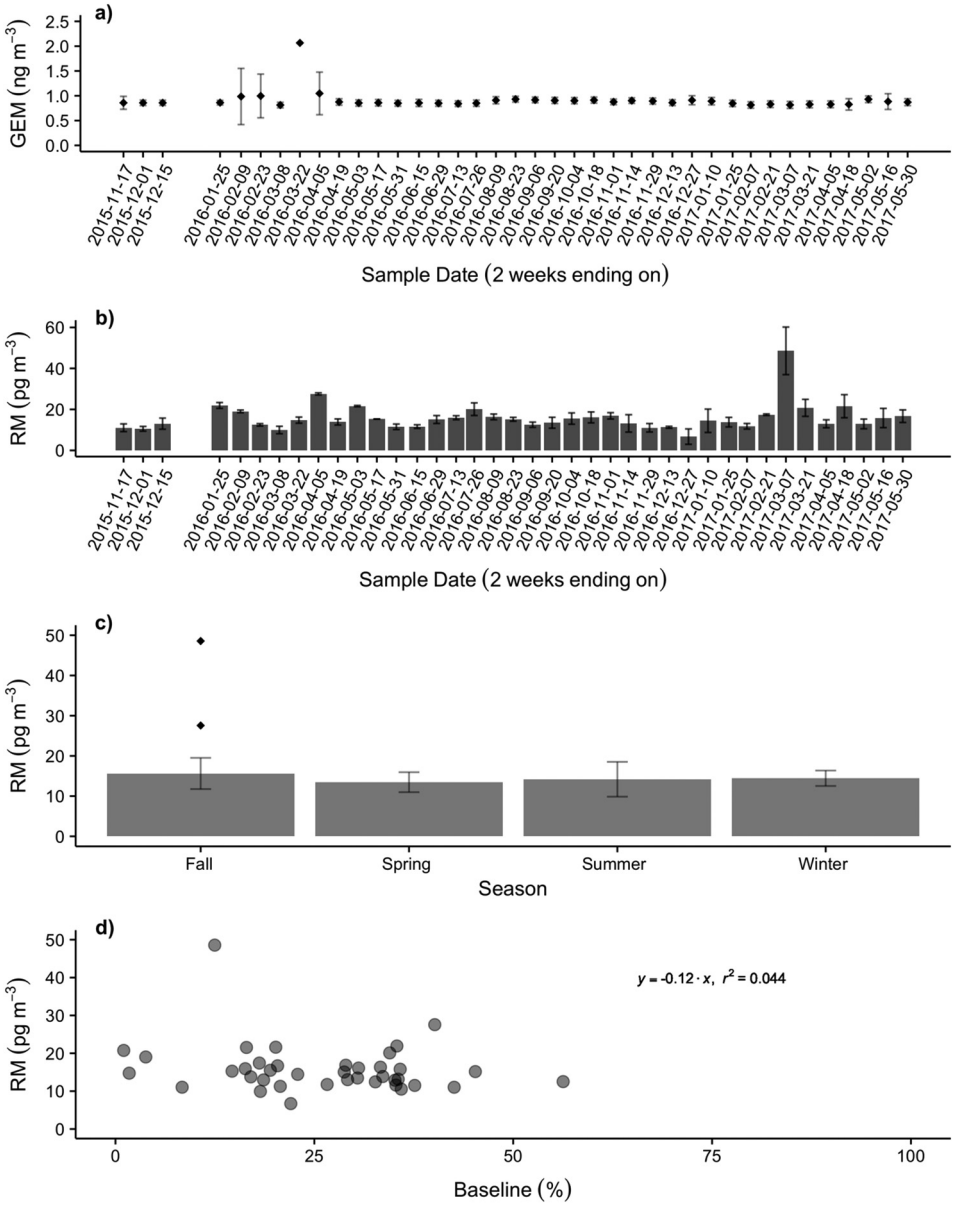

Fig. 3. Atmospheric Hg at CGBAPS for a) 2-week GEM sample means, b) 2-week RM sample means, c) seasonal averages of RM, and d) RM in relation to percent of sampled air from baseline wind sector (190–280°). Where shown, error bars = standard deviation.

oxidative production of RM, especially as both events occurred over night when photochemical oxidation would be at its lowest.

The 2-week sample periods ending March 22 and April 5, 2016, experienced even higher mean GEM concentrations of 2.1 ± 1.9 and 1.1 ± 0.4 ng m^{-3} due to a significant and extended plume event (Fig. 3a). Peak 5-min GEM concentrations rose to ~12 ng m^{-3} on March 17 and remained elevated (>2.0 ng m^{-3}) until March 23, bracketing the two filter deployment periods. This event is attributable to a renewed flair-up of bushfire activity due south of the station, beginning March 16 and peaking on March 17. Back trajectory calculations during this period show arriving air masses traveling directly over the burn area, in addition to burn areas farther south (SI Fig. 4). The RM concentration for the sample period ending March 22 was not exceptional (15 ± 2 pg m^{-3}). However, during the following sample period ending April 5, mean RM concentration was 28 ± 1 pg m^{-3}, the second highest value recorded at CGBAPS, possibly due to an aging and oxidized plume chemistry in the sample further removed in time from primary combustion.

The highest recorded 2-week RM concentration of 48 pg m^{-3} occurred in a period of no major bushfire activity (Feb. 21 – March 7, 2017). This sample period and the next (also above average RM at 21 pg m^{-3}, March 7 to March 21, 2017) were dominated by air flow from the east (75–105°, 42 and 51% of hourly wind directions, respectively), unusual for the CGBAPS site. Back trajectory analysis confirms the easterly flow during this period, with a preponderance of trajectories arriving from the east after traveling over the Bass Straight below 1000 m, well within the mixed depth layer (Fig. 4a). An iron ore smelting plant (Grange Corp. Port Latta Facility) is located ~61.5 km away from CGBAPS at 108° east bearing, and is a modest source of Hg and RM (5.2 kg y-1, NPI, 2017). Shipping through the Bass Straight to the east-northeast of the site may also be a contributing source during these east wind periods, similar to an observation made by Sprovieri et al. (2010) for high RM events in the Mediterranean MBL. A similar flow regime was also apparent for the following sample period March 7 to March 21 (Fig. 4b).

3.4. Reactive Hg at Macquarie University Automatic Weather Station

In general, the MQAWS site was hotter and more humid than CGBAPS. The median temperature was 17.3 °C (range −0.8 to

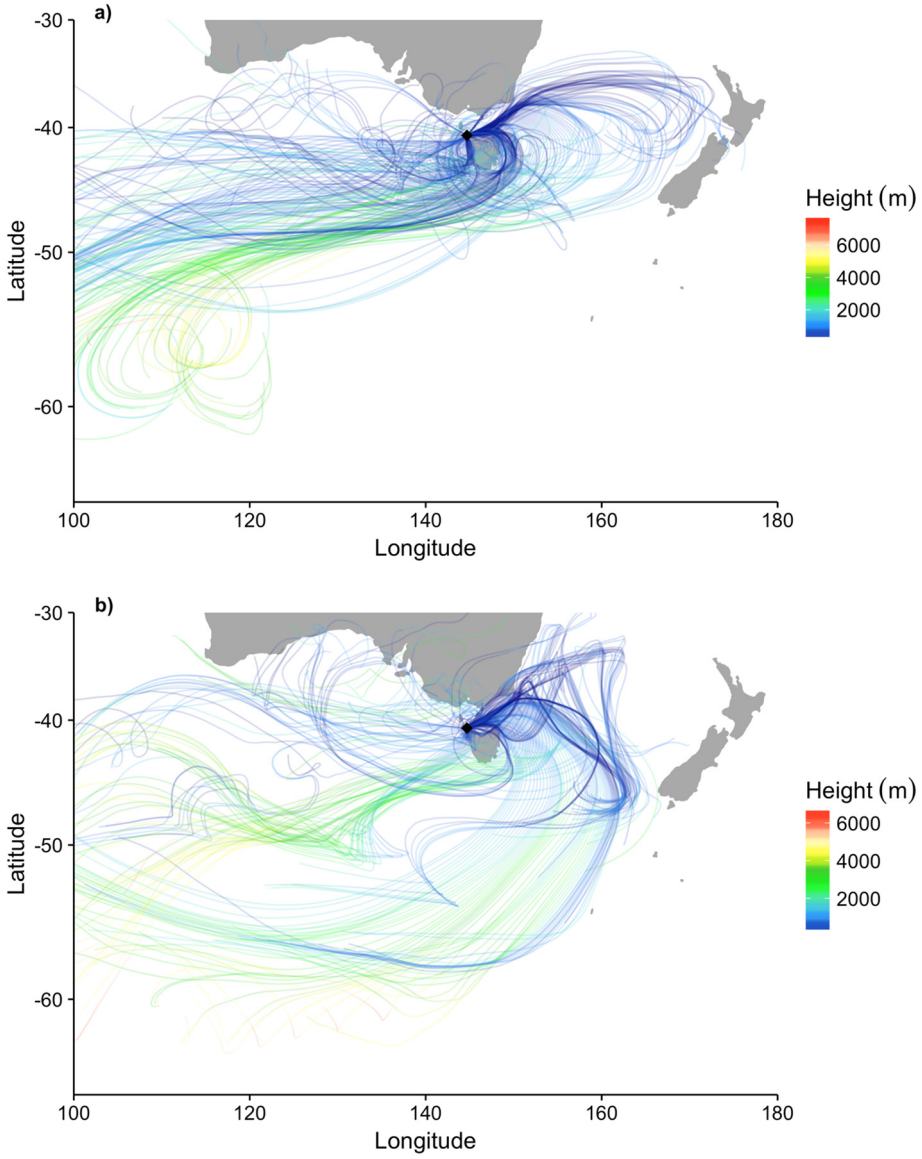

Fig. 4. Ensemble of 120 h back trajectory plots for air arriving at CGBAPS during a) Feb. 21 – March 7, 2017 and b) March 7–21, 2017. Trajectories initiated hourly from a single point above station with height of 0.5× mixed layer depth.

42.2 °C), and the median RH was 85% (range 21 to 100%). As is evident from the range in temperature and RH, the site also experienced more variability in meteorology compared to the more moderated climate at CGBAPS. Total rainfall in 2016 was above average at 1316.4 mm (annual median total 1122.1 mm). Overall wind velocities were generally low at the MQAWS site, and the dominant wind direction was from the west-northwest (225–345°), except during the summer sea breeze from the east-southeast (SI Fig. 6).

Seasonally, the lowest mean RM concentrations occurred in the summer (13 ± 4 pg m^{-3}, $n = 7$) and the highest RM concentrations occurred in the winter (22 ± 7 pg m^{-3}, n = 7), a statistically significant difference (Welch *t*-test, $p = .015$, Fig. 5c). Mean RM concentrations during the fall and spring were intermediate between the summer and winter extremes and were not significantly different. As with CGBAPS, mean 2-week RM concentrations were compared to mean 2-week concentrations of GEM, median values of temperature, RH, barometric pressure, and wind speed, as well as total 2-week precipitation (SI Fig. 7), and no relationship was discernible at the 2-week temporal resolution (r^2 values <0.1).

The difference between summer and winter RM concentrations at MQAWS appears to be largely a function of different air masses between seasons. The relatively high winter RM is associated with ~50% of air flow originating from the west and northwest (SI Fig. 6b), a direction that is entirely terrestrial, with varying degrees of urban and industrial development. The majority of significant point source Hg emissions in the Sydney Basin are to the west and south of the MQAWS site, primarily from municipal waste processing, power generation, and refining, with total Hg emissions of 43.7 kg in the 2016/2017 reporting period (SI Fig. 8).

Back trajectory calculations for the 2-week sample period with the highest observed RM concentration at MQAWS (33 ± 4 pg m^{-3}, July 11–25, 2016) demonstrated that a majority of air masses traveled over wide areas of the continent and passed over the urban/industrial areas of western Sydney before reaching the site from the western quadrant (Fig. 6a). It is likely that in sample periods with this general source area scenario, terrestrial and point source emissions contribute to enhanced RM concentrations.

In contrast to winter patterns, prevailing summertime easterly winds (SI Fig. 6a) originated from maritime air and traveled a relatively brief distance over land and the less dense suburban neighborhoods of Northern Sydney, an area with no significant Hg source emissions. The lowest observed RM concentration at MQAWS (7 ± 1 pg m^{-3}) occurred

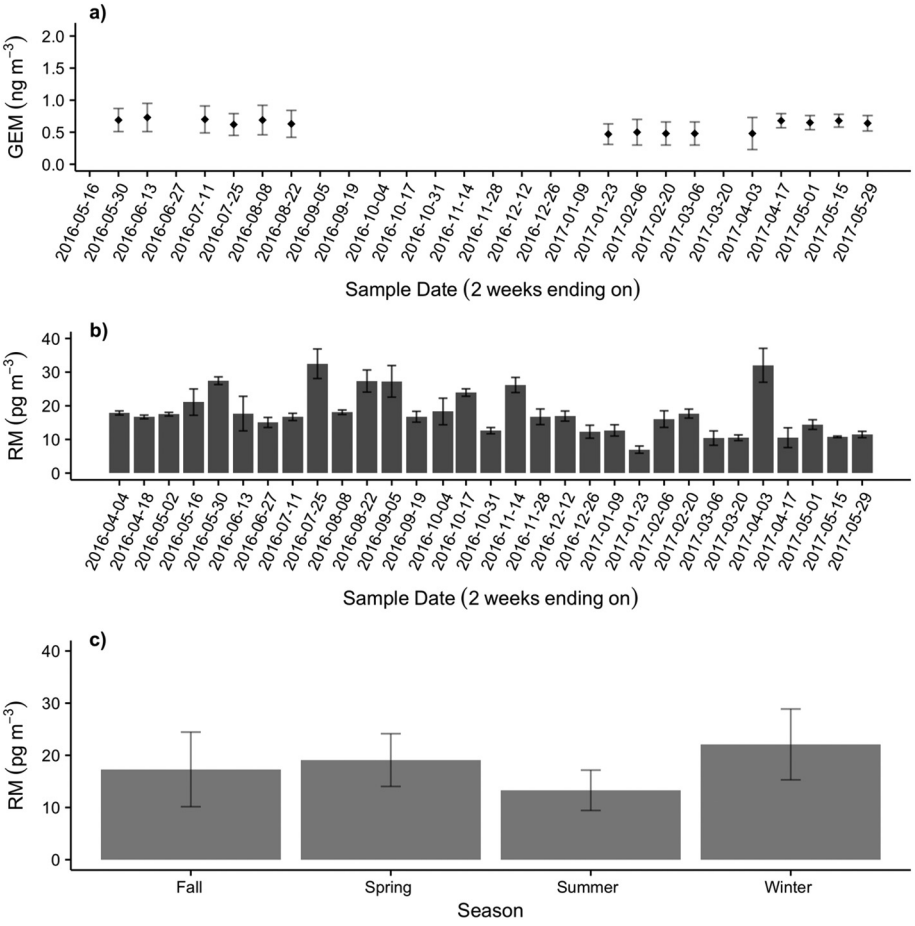

Fig. 5. Atmospheric Hg at MQAWS for a) 2-week GEM sample means, b) 2-week RM sample means, and c) seasonal averages of RM. error bars = standard deviation.

in the summer sample period January 9–23, 2017. Back trajectory calculations for this period confirm that air arrived at the site predominantly from the eastern quadrant, having passed through the MBL over the Southern Ocean and Tasman Sea, though a minority of trajectories arrived from a southerly direction (Fig. 6b).

3.5. Reactive Hg on RV investigator research voyage

CEM filters were deployed on RVI during an extended research voyage to the East Antarctic coast from January 10 to March 4, 2017. The mean hourly GEM concentration over the entire voyage was 0.5 ± 0.1 ng m^{-3} (n = 978) and ranged from 0.2 to 0.8 ng m^{-3} (Fig. 7). GEM concentrations were distinctly and significantly lower (0.4 ± 0.05 ng m^{-3}, n = 134, Welch *t*-test, $p < .000$) between 43.5 and 53.5° south latitude compared to the voyage as a whole, for both the outbound and return segments of the voyage. The mean RM concentration over all deployments was 24 ± 7 pg m^{-3} (n = 4). The mean CEM filter blank was 26 ± 9 pg, resulting in an average MDL of 2 pg m^{-3} for a 2-week sample period, which all filter measurements were well above.

The first filter deployment (January 10–26) included four days in the port of Hobart before the voyage south began at approximately 18:00 ship's time, January 14, and so is somewhat compromised by the port environment. The second and third 2-week CEM filter deployments occurred while RVI was on station off the East Antarctic coast between 113 and 122°east longitude (ship track and GEM shown SI Figs. 9 and 10), and these samples can be considered Antarctic background. Mean RM concentrations were 33 ± 3 pg m^{-3} (n = 3) in the first 2 weeks, and 22 pg m^{-3} (21.2 to 22.3 pg m^{-3}, n = 2) in the following 2 weeks. The final filter deployment included the transit back to port and was relatively low at 16 ± 3 pg m^{-3}.

Mean hourly GEM concentrations were variable (0.2 to 0.9 ng m^{-3}) and on average significantly higher while off the East Antarctic coast (0.6 ± 0.1 ng m^{-3}, n = 568, Welch t-test, $p < .000$), relative to the overall voyage. An apparent GEM hotspot with hourly concentrations above 0.8 ng m^{-3} was observed around coordinates −64.3 S 117.5 W, during two different transects of the area (January 28 and February 13). Elevated GEM concentrations were also only strongly evident at midday (10,00 - 16,00) during these events, which may indicate a diurnal GEM source mechanism. Back trajectories initiated from RVI's position in the GEM hotspot area on January 28 indicated air masses originating over the Ross Sea and traveling at low altitude along the East Antarctic coast and the Dumont d'Urville Sea (SI Fig. 11). This is not easily classifiable as either a maritime or continental air source. Back trajectories from the February 13 GEM enhancement arrive from multiple directions in a cyclonic spiral indicative of a SH low-pressure system (SI Fig. 12). The RVI ship's log confirms storm conditions on February 12–13. It is difficult to ascertain a definite source region for this period, but some of the back trajectories follow the same coastal path as during the January 28 GEM enhancement, and it may be that these two events result from related sources.

Along the region of the Antarctic coast visited by the RV Investigator, previous observations at Dumont d'Urville Station have demonstrated high variability in summertime GEM concentrations (0.1 to 3.6 ng m^{-3}), attributed to variations between marine and continental source air, as well as possible diurnal enhancements in GEM concentration due to emissions from snow and ornithogenic (penguin guano) soil surfaces (Angot et al., 2016a; Angot et al., 2016b). In-situ oxidation of GEM to RM is thought to be comparatively low in this region of Antarctica due to less extensive sea ice cover, and therefore a lower abundance of available reactive bromine molecules, resulting in less

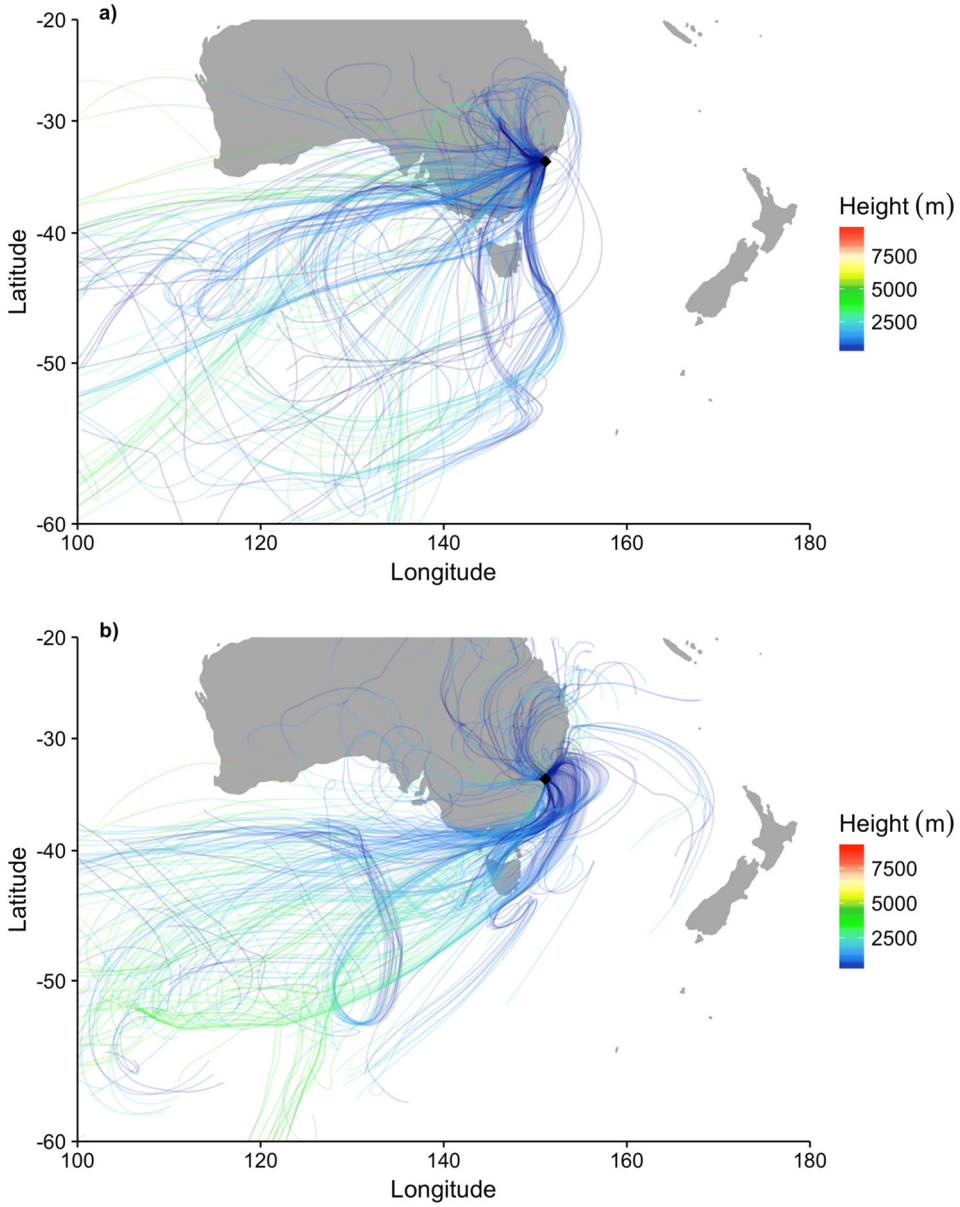

Fig. 6. Ensemble of 120 h back trajectory plots for air arriving at MQAWS during a) representative winter period (July 11–25, 2016) and b) a representative summer period (January 9–23, 2017). Trajectories initiated hourly from a single point above station with height of 0.5× mixed layer depth.

efficient oxidative bromine chemistry. Angot et al. (2016b) speculated that air enriched in RM species reaches the Dumont d'Urville coast from the high interior Antarctic plateau, where GEM is oxidized in-situ through efficient OH/NOx chemistry. The relatively high RM concentrations measured on RVI may be attributable to a similar transport mechanism from the continental interior that corresponds with the voyage sections where GEM was depleted. Unfortunately, given the long 2-week RM sample time, it is impossible to know without finer resolution exactly when and where in the voyage track the elevated RM concentrations occurred.

3.6. Overall cation exchange membrane performance

Mean RM breakthrough to the secondary CEM filters was 21.1 ± 9.5% (n = 114) at CGBAPS and 17.8 ± 9.9% (n = 92) at MQAWS. These rates of RM breakthrough were statistically significantly different (Welch *t*-test, $p = .01$). At each site, comparison of 2-week median breakthrough values to corresponding 2-week mean concentrations of GEM, median values of temperature, RH, barometric pressure, wind speed, and total 2-week precipitation revealed no correlation. However, MQAWS was overall hotter and more humid than the CGBAPS site, and it is possible this contributed to the slightly higher mean rates of RM breakthrough. During the RVI voyage, mean RM breakthrough to the secondary filters was 19.1 ± 5.1% ($n = 10$), very similar to breakthrough at the ground-based monitoring sites. The voyage was generally cooler, but more humid than at either ground site.

There has been speculation that humidity in particular might have an impact on RM collection and possible breakthrough on the CEM material (Huang and Gustin, 2015). Though humidity has not been shown to affect RM breakthrough on CEM filters loaded with a pure GOM compound ($HgBr_2$) in clean, particle-free laboratory air (Miller et al., 2019), the effects of RH in ambient air remain unclear. We hypothesized that in ambient air, PBM larger than the CEM pore size (0.8 μm) would be collected and, reacting with other atmospheric constituents such as water vapor, potentially volatilized from the primary filter surface as a gas-phase reactive Hg species, escaping to the secondary filter as breakthrough. However, a comparison of total particle counts in each sample period versus mean % RM breakthrough failed to reveal any relationship

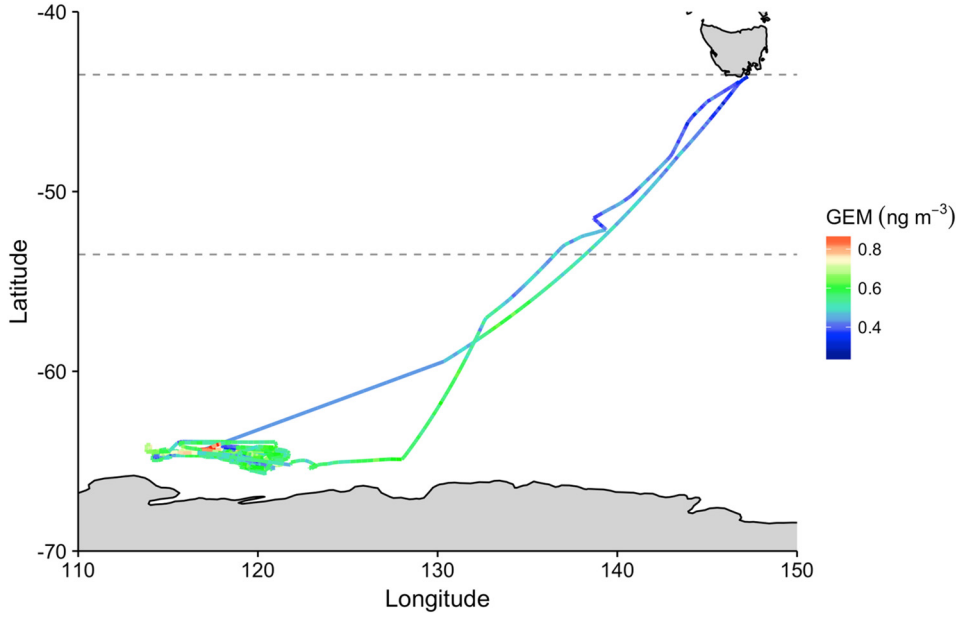

Fig. 7. Hourly GEM concentrations along course of RVI voyage in Southern Ocean, January 14 – March 4, 2017. Low GEM values between −43.5 and −53.5 latitudes bracketed by dashed lines. Periods of no data indicated by grey line segments.

(SI Fig. 13, $r^2 < 0.000$). Since particle counts included everything down to 0.0025 μm, a more selective count at sizes larger than the filter pore size might be more relevant.

4. Discussion

Up to 54% of total atmospheric Hg in the Southern Hemisphere is thought to be derived from evasion of Hg^0 from the ocean surface, which is balanced by daytime photo-chemical oxidation to Hg^{2+} and subsequent deposition of resulting RM compounds back to the ocean (Laurier and Mason, 2007; Mason and Sheu, 2002; Strode et al., 2007). The formation of RM within the MBL is generally thought to be dominated by Br oxidation processes (Hedgecock and Pirrone, 2001; Hedgecock et al., 2003; Holmes et al., 2009; Horowitz et al., 2017; Laurier and Mason, 2007; Laurier et al., 2003; Sprovieri et al., 2010; Sprovieri et al., 2002). A large part of RM within the MBL is also believed to be bound with coarse sea-salt aerosols up to 10 μm in size (Feddersen et al., 2012; Holmes et al., 2009; Malcolm and Keeler, 2007; Talbot et al., 2011).

Few speciated atmospheric Hg measurements have been made in the Southern Hemisphere, with only one year-long continuous data set from Amsterdam Island (Angot et al., 2014), supplemented by shorter term campaign studies in Antarctica (Angot et al., 2016a; Brooks et al., 2008b; Sprovieri et al., 2002; Temme et al., 2003), and a few oceanic research voyages (Angot et al., 2016a; Soerensen et al., 2010; Temme et al., 2003). A major limitation to continuous speciated Hg measurements in the Southern Hemisphere has been suitable site and logistical arrangements for operation of the full Tekran® 2537/1130/1135 speciation system. Furthermore, the demonstrated low measurement bias for GOM and PBM raises concerns about potential under quantification of total RM using the Tekran® system.

Many studies using the Tekran® speciation system at MBL locations report very low GOM and PBM concentrations (Table 1). Angot et al. (2014) reported average GOM and PBM concentrations of <1 pg m^{-3} for Amsterdam Island, with measurements frequently below detection, similar to many other coastal ground-based RM measurements in the MBL (Chand et al., 2008; Huang et al., 2013; Marumoto et al., 2015; Wang et al., 2014; Weiss-Penzias et al., 2003; Wright et al., 2014). An exception is the study of Fu et al. (2018), where measurements made in the MBL on Huaniao Island in the East China Sea resulted in relatively large mean concentrations of GOM (8 ± 10 pg m^{-3}) and PBM (26 ± 38 pg m^{-3}), with peak concentrations up to 422 and 97 pg m^{-3}, respectively. However, Fu et al. (2018) attribute pollution outflow from mainland China as the major source of atmospheric Hg at the site. Data acquired on a circumnavigational voyage measuring atmospheric GEM and GOM using just the Tekran® 2537/1130, suggested a global mean GOM concentration of 3.1 ± 11 pg m^{-3} in the MBL (4.3 ± 0.14 pg m^{-3} for the SH MBL, Soerensen et al. (2010), in general agreement with other voyage data of 2 to 10 pg m^{-3} (Laurier et al., 2003; Temme et al., 2003).

Table 1
Average GEM and RM concentrations measured using the Tekran® speciation system at select marine boundary layer locations around the Indo-Pacific. MDL is method detection limit.

Location & elevation	Coordinates	Duration	GEM (ng m^{-3})	GOM (pg m^{-3})	PBM (pg m^{-3})	Reference
Coastal/marine boundary layer						
Cheeka Peak Obs., USA (492 m)	48.299 N 124.626 W	Sept. 2001 - May 2002	1.55 ± 0.13	MDL - 1.6	MDL - 0.5	Weiss-Penzias et al., 2003
Elkhorn Slough, USA (16 m)	36.819 N 121.736 W	March 2011 - Nov. 2011	1.40 ± 0.2	0.5 ± 1.2	4 ± 5	Wright et al., 2014
		March 2012–April 2012	na	1.4 ± 1.0	3.6 ± 1.8	Huang et al., 2013
Fukuoka, Japan (20 m)	33.548 N 130.364 E	June 2012–May 2013	2.33 ± 0.49	5.7 ± 9.4	10 ± 11	Marumoto et al., 2015
Huaniao Island, China (70 m)	30.861 N 122.673 E	Oct. 2013 - Jan. 2014	2.25 ± 1.03	26 ± 38	8 ± 10	Fu et al., 2018
Cape Hedo Obs., Japan (20 m)	26.872 N 128.263 E	March 2004–May 2004	2.04 ± 0.38	4.5 ± 5.4	3.0 ± 2.5	Chand et al., 2008
Galapagos Islands (5 m)	−0.959 S 90.963 W	Feb. 2011 - Oct. 2011	1.08 ± 0.17	MDL - 3.8	MDL - 1.1	Wang et al., 2014
Amsterdam Island (50 m)	−37.796 S 77.551 E	Jan. 2012 - Dec. 2013	1.03 ± 0.08	MDL - 4.1	MDL - 12.7	Angot et al., 2014
Sydney, Australia (64 m)	−33.765 S 151.117 E	April 2016–May 2017	0.65 ± 0.24	17.8 ± 6.6 (RM)		This study
Cape Grim, Australia (94 m)	−40.683 S 144.690 E	Nov. 2015 - May 2017	0.90 ± 0.35	15.9 ± 6.7 (RM)		This study

The explanation for these low RM concentrations in the MBL has been rapid deposition of the RM formed by in-situ oxidation processes, due to scavenging by abundant sea-spray and sea-salt aerosols (Laurier et al., 2003; Mason and Sheu, 2002; Sommar et al., 2010). Some studies have reported much larger RM concentrations in or associated with MBL air, but these are in the minority of observations (Mason et al., 2001; Timonen et al., 2013). There are other scenarios with significant in-situ oxidation of GEM in which the resulting enhancement of RM is typically observable, e.g. coastal polar locations during springtime Atmospheric Mercury Depletion Events (Steffen et al., 2008, 2013). Like in the MBL environment, RM formed in polar AMDEs is also thought to rapidly deposit, though more so to ice surfaces than marine aerosols (Angot et al., 2016a; Brooks et al., 2008a; Steffen et al., 2002), yet elevated atmospheric RM concentrations are still measured in spite of high rates of deposition. Why then are the observations of RM in the MBL so modest, or even undetectable? We posit that the low RM measurement bias demonstrated on the Tekran® 1130 system in previous studies (Ambrose et al., 2013; Lyman et al., 2010; McClure et al., 2014) may be contributing to artificially low observations of RM in the MBL, due to the demonstrated low-collection bias of the KCl denuder in humid conditions, and also at least in part to the exclusion of all particles larger than the 2.5 μm cut-point on the Tekran® inlet.

In this study, long term measurements at two coastal sites resulted in baseline MBL RM concentrations of 13 ± 4 pg m^{-3} (MQAWS during summer maritime flow regime) and 13 ± 2 pg m^{-3} (CGBAPS, maritime baseline sector). The one sample period onboard RVI that can definitely be considered entirely oceanic without continental influence showed an RM concentration of 16 ± 3 pg m^{-3}. Thus, a range of 10 to 20 pg m^{-3} may be more representative of average RM concentrations for MBL air around southeastern Australia.

In a recent study using the UNR CEM filter method, Luippold et al. (2020b) report RM concentrations measured at 3 locations in the continental United States, and from Mauna Loa Global Atmospheric Observatory (at 3396 m a.s.l) in the Hawai'ian Islands. From west to east across the continent, RM concentrations in Nevada were 60 ± 40 pg m^{-3}, 38 ± 4 pg m^{-3} in Utah, and 17 ± 2 pg m^{-3} in Maryland, while at Mauna Loa RM concentrations averaged 133 ± 5 pg m^{-3}. Luippold et al. (2020b) demonstrated that each location was influenced by different atmospheric Hg oxidants and sources. Mauna Loa sometimes receives upslope air flow from the MBL, but experiences subsiding free tropospheric air nightly. We suggest the generally much higher RM concentrations observed by Luippold et al. (2020b) are due to greater Hg contamination of the NH and its oceans.

5. Conclusions

Reactive Hg concentrations were relatively uniform between the CGBAPS and MQAWS sites, averaging around 16 and 18 pg m^{-3}, respectively, and ranging from 6 to 48 pg m^{-3}. RM concentrations measured on the RVI voyage in the Southern Ocean were in a similar range (16–32 pg m^{-3}) as the ground-based sites. These results suggest that RM concentrations are relatively stable, likely due to a semi-steady-state equilibrium between in-situ formation and depositional processes within the MBL, as suggested in other studies. However, total RM concentrations measured in this study (overall average 19 pg m^{-3}) were somewhat higher than concentrations reported for the MBL in many previous studies (~2 to 10 pg m^{-3} total RM). We believe this may be explained by the collection of PBM associated with all sea-salt aerosols larger than the CEM filter pore size of 0.8 μm, versus exclusion of coarse aerosols >2.5 μm by the conventional Tekran® 2537/1130/1135 speciation system.

No samples were below detection limit at the 2-week temporal resolution of the filter samples. In this study there was no discernible correlation between either RM collection or RM breakthrough with humidity or any other measured environmental parameter, including total particle counts at CGBAPS. The mechanism of RM breakthrough in ambient air CEM samples remains unclear, though greater size-selectivity in particle count analysis could be potentially illuminating.

At CGBAPS there was no meaningful seasonal variation in RM concentrations, though isolated periods were occasionally notably higher or lower than average. Widespread bushfire activity in Tasmania and near the CGBAPS site was the largest source of variation in both GEM and RM concentrations, but was highly atypical. The overall lack of variation in RM concentration at CGBAPS is likely attributable to the background marine environment, with generally mild conditions, relatively consistent source air, and constant RM source concentrations formed in-situ in the MBL.

In contrast to CGBAPS, the MQAWS site experienced statistically higher RM concentrations in the winter versus the summer. During the summer months, air masses predominantly arrived from the MBL to the east and southeast, versus the prevalence of a northwesterly wind in the winter arriving from terrestrial surfaces. These summertime maritime RM concentrations at MQAWS were comparable to baseline RM concentrations at CGBAPS, suggesting uniform MBL RM concentrations in coastal Australian waters.

High variability in GEM concentrations and elevated RM concentrations were observed from the RV Investigator on transects immediately off the East Antarctic coast. Though in a similar overall range, average RM concentrations off the Antarctic coast were somewhat higher than at the ground-based temperate coastal measurement sites at CGBAPS and MQAWS. The high variability in GEM concentrations (0.2 to 0.9 ng m^{-3}) is in-line with other observations from the East Antarctic coast, and the relatively high RM concentrations may be due to Antarctic continental outflow.

The RM concentrations measured in this study using the CEM filter-based method are higher relative to most other measurements in the MBL using the Tekran® 2537/1130/1135 Speciation System, and this may have important implications for accurately depicting total Hg concentrations in global ocean-atmosphere models.

CRediT authorship contribution statement

Matthieu B. Miller: Conceptualization, Investigation, Methodology, Data curation, Formal analysis, Validation, Visualization, Writing - original draft, Writing - review & editing. **Dean A. Howard:** Methodology, Data curation, Formal analysis, Writing - review & editing. **Ashley M. Pierce:** Methodology, Data curation, Formal analysis, Writing - review & editing. **Kellie R. Cook:** Data curation, Formal analysis, Writing - review & editing. **Melita Keywood:** Resources, Funding acquisition, Writing - review & editing. **Jennifer Powell:** Resources, Writing - review & editing. **Mae S. Gustin:** Conceptualization, Funding acquisition, Supervision, Writing - original draft, Writing - review & editing. **Grant C. Edwards:** Conceptualization, Funding acquisition, Supervision, Writing - original draft, Writing - review & editing.

Declaration of competing interest

The authors declare that they have no known competing financial interests or personal relationships that could have appeared to influence the work reported in this paper.

Acknowledgements

The authors would like to acknowledge funding from Macquarie University iMQRES 2015148 and NSF Grant 629679. The authors also thank the students and staff of Dr. Gustin's research group at the University of Nevada Reno, and Dr. Edwards' research group at Macquarie University. Thanks goes to RVI voyage volunteer Jack Simmons for assistant with sample collection. Continued support for the Cape Grim Program from the Australian Bureau of Meteorology and Commonwealth Scientific and Industrial Research Organization (CSIRO) and the personal effort of the outstanding Cape Grim support

staff maintaining equipment and collecting samples is gratefully acknowledged. We all bid an untimely farewell to Dr. Grant C. Edwards, who was ever a cheerful friend, mentor, and colleague. Dr. Edwards passed away unexpectedly on September 10, 2018.

Appendix A. Supplementary data

Supplementary data to this article can be found online at https://doi.org/10.1016/j.scitotenv.2020.141681.

References

Ambrose, J.L., Lyman, S.N., Huang, J., Gustin, M.S., Jaffe, D.A., 2013. Fast time resolution oxidized mercury measurements during the Reno atmospheric mercury intercomparison experiment (RAMIX). Environmental Science & Technology 47, 7285–7294.

Angot, H., Barret, M., Magand, O., Ramonet, M., Dommergue, A., 2014. A 2-year record of atmospheric mercury species at a background southern hemisphere station on Amsterdam Island. Atmos. Chem. Phys. 14, 11461–11473.

Angot, H., Dastoor, A., De Simone, F., Gårdfeldt, K., Gencarelli, C.N., Hedgecock, I.M., et al., 2016a. Chemical cycling and deposition of atmospheric mercury in polar regions: review of recent measurements and comparison with models. Atmos. Chem. Phys. 16, 10735–10763.

Angot, H., Dion, I., Vogel, N., Legrand, M., Magand, O., Dommergue, A., 2016b. Multi-year record of atmospheric mercury at Dumont d'Urville, East Antarctic coast: continental outflow and oceanic influences. Atmos. Chem. Phys. 16, 8265–8279.

Brooks, S., Arimoto, R., Lindberg, S., Southworth, G., 2008a. Antarctic polar plateau snow surface conversion of deposited oxidized mercury to gaseous elemental mercury with fractional long-term burial. Atmos. Environ. 42, 2877–2884.

Brooks, S., Lindberg, S., Southworth, G., Arimoto, R., 2008b. Springtime atmospheric mercury speciation in the McMurdo, Antarctica coastal region. Atmos. Environ. 42, 2885–2893.

Chand, D., Jaffe, D., Prestbo, E., Swartzendruber, P.C., Hafner, W., Weiss-Penzias, P., et al., 2008. Reactive and particulate mercury in the Asian marine boundary layer. Atmos. Environ. 42, 7988–7996.

Cheng, I., Zhang, L., 2017. Uncertainty assessment of gaseous oxidized mercury measurements collected by atmospheric mercury network. Environmental Science & Technology 51, 855–862.

Draxler, R., Hess, G., 1998. An overview of the HYSPLIT_4 modelling system for trajectories, dispersion on and deposition. Aust. Meteorol. Mag. 47, 295–308.

Ebinghaus, R., Kock, H.H., Temme, C., Einax, J.W., Löwe, A.G., Richter, A., et al., 2002. Antarctic springtime depletion of atmospheric mercury. Environmental Science & Technology 36, 1238–1244.

Feddersen, D.M., Talbot, R., Mao, H., Sive, B.C., 2012. Size distribution of particulate mercury in marine and coastal atmospheres. Atmos. Chem. Phys. 12, 10899–10909.

Finley, B.D., Swartzendruber, P.C., Jaffe, D.A., 2009. Particulate mercury emissions in regional wildfire plumes observed at the Mount Bachelor Observatory. Atmos. Environ. 43, 6074–6083.

Fu, X., Yang, X., Tan, Q., Ming, L., Lin, T., Lin, C.J., et al., 2018. Isotopic composition of gaseous elemental mercury in the marine boundary layer of East China Sea. Journal of Geophysical Research: Atmospheres 123, 7656–7669.

Gustin, M., Jaffe, D., 2010. Reducing the uncertainty in measurement and understanding of mercury in the atmosphere. Environmental Science & Technology 44, 2222–2227.

Gustin, M.S., Amos, H.M., Huang, J., Miller, M.B., Heidecorn, K., 2015. Measuring and modeling mercury in the atmosphere: a critical review. Atmos. Chem. Phys. 15, 5697–5713.

Gustin, M.S., Pierce, A.M., Huang, J., Miller, M.B., Holmes, H.A., Loria-Salazar, S.M., 2016. Evidence for different reactive Hg sources and chemical compounds at adjacent valley and high elevation locations. Environmental Science & Technology 50, 12225–12231.

Gustin, M.S., Dunham-Cheatham, S.M., Zhang, L., 2019. Comparison of 4 methods for measurement of reactive gaseous oxidized, and particulate bound mercury. Environ. Sci. Technol. 53 (24), 14489–14495. https://doi.org/10.1021/acs.est.9b04648.

Hedgecock, I., Pirrone, N., 2001. Mercury and photochemistry in the marine boundary layer-modelling studies suggest the in situ production of reactive gas phase mercury. Atmos. Environ. 35, 3055–3062.

Hedgecock, I., Pirrone, N., Sprovieri, F., Pesenti, E., 2003. Reactive gaseous mercury in the marine boundary layer: modelling and experimental evidence of its formation in the Mediterranean region. Atmos. Environ. 37, S41–S49.

Holmes, C.D., Jacob, D.J., Mason, R.P., Jaffe, D.A., 2009. Sources and deposition of reactive gaseous mercury in the marine atmosphere. Atmos. Environ. 43, 2278–2285.

Horowitz, H., Jacob, D., Zhang, Y., Dibble, T., Slemr, F., Amos, H., et al., 2017. A new mechanism for atmospheric mercury redox chemistry: implications for the global mercury budget. Atmos. Chem. Phys. 17, 6353–6371.

Howard, D., 2018. Aspects of the Biogeochemical Cycling of Mercury in Australia and the Southern Hemisphere. Department of Environmental Science. PhD. Macquarie University, Sydney, Australia, p. 160.

Howard, D., Macsween, K., Edwards, G.C., Desservettaz, M., Guérette, E.-A., Paton-Walsh, C., et al., 2019. Investigation of mercury emissions from burning of Australian eucalypt forest surface fuels using a combustion wind tunnel and field observations. Atmos. Environ. 202, 17–27.

Huang, J., Gustin, M.S., 2015. Uncertainties of gaseous oxidized mercury measurements using KCl-coated denuders, cation-exchange membranes, and nylon membranes: humidity influences. Environmental Science & Technology 49, 6102–6108.

Huang, J., Miller, M.B., Weiss-Penzias, P., Gustin, M.S., 2013. Comparison of gaseous oxidized Hg measured by KCl-coated denuders, and nylon and cation exchange membranes. Environmental Science & Technology 47, 7307–7316.

Huang, J., Miller, M.B., Edgerton, E., Sexauer Gustin, M., 2017. Deciphering potential chemical compounds of gaseous oxidized mercury in Florida, USA. Atmos. Chem. Phys. 17, 1689–1698.

Jaffe, D.A., Lyman, S., Amos, H.M., Gustin, M.S., Huang, J., Selin, N.E., et al., 2014. Progress on understanding atmospheric mercury hampered by uncertain measurements. Environmental Science & Technology 48, 7204–7206.

Landis, M.S., Stevens, R.K., Schaedlich, F., Prestbo, E.M., 2002. Development and characterization of an annular denuder methodology for the measurement of divalent inorganic reactive gaseous mercury in ambient air. Environmental Science & Technology 36, 3000–3009.

Laurier, F., Mason, R., 2007. Mercury concentration and speciation in the coastal and open ocean boundary layer. J. Geophys. Res.-Atmos. 112.

Laurier, F., Mason, R., Whalin, L., Kato, S., 2003. Reactive gaseous mercury formation in the North Pacific Ocean's marine boundary layer: a potential role of halogen chemistry. J. Geophys. Res.-Atmos. 108.

Luippold, A., Gustin, M.S., Dunham-Cheatham, S.M., Zhang, L., 2020b. Improvement of quantification and identification of atmospheric reactive mercury. Atmospheric Environment 2020b 224, 117307. https://doi.org/10.1016/j.atmosenv.2020.117307 1 March.

Luippold, A., Gustin, M.S., Dunham-Cheatham, S.M., Castro, M., Luke, W., Lyman, S., Zhang, L., 2020a. Use of multiple lines of evidence to understand reactive mercury concentrations and chemistry in Hawaii, Nevada, Maryland, and Utah, USA. Environ. Sci. Technol. https://doi.org/10.1021/acs.est.0c02283.

Lyman, S.N., Jaffe, D.A., Gustin, M.S., 2010. Release of mercury halides from KCl denuders in the presence of ozone. Atmos. Chem. Phys. 10, 8197–8204.

Lyman, S., Jones, C., O'Neil, T., Allen, T., Miller, M., Gustin, M.S., et al., 2016. Automated calibration of atmospheric oxidized mercury measurements. Environmental Science & Technology 50, 12921–12927.

Malcolm, E.G., Keeler, G.J., 2007. Evidence for a sampling artifact for particulate-phase mercury in the marine atmosphere. Atmos. Environ. 41, 3352–3359.

Marumoto, K., Hayashi, M., Takami, A., 2015. Atmospheric mercury concentrations at two sites in the Kyushu Islands, Japan, and evidence of long-range transport from East Asia. Atmos. Environ. 117, 147–155.

Marusczak, N., Sonke, J.E., Fu, X., Jiskra, M., 2017. Tropospheric GOM at the pic du Midi observatory—correcting Bias in denuder based observations. Environmental Science & Technology 51, 863–869.

Mason, R.P., Sheu, G.R., 2002. Role of the ocean in the global mercury cycle. Glob. Biogeochem. Cycles 16, 40–1–40–14.

Mason, R.P., Lawson, N.M., Sheu, G.R., 2001. Mercury in the Atlantic Ocean: factors controlling air–sea exchange of mercury and its distribution in the upper waters. Deep-Sea Res. II Top. Stud. Oceanogr. 48, 2829–2853.

McClure, C.D., Jaffe, D.A., Edgerton, E.S., 2014. Evaluation of the KCl denuder method for gaseous oxidized mercury using HgBr2 at an in-service AMNet site. Environmental Science & Technology 48, 11437–11444.

Miller, M.B., Fine, R., Pierce, A.M., Gustin, M.S., 2015. Identifying sources of ozone to three rural locations in Nevada, USA, using ancillary gas pollutants, aerosol chemistry, and mercury. Sci. Total Environ. 530-531, 483–492.

Miller, M.B., Dunham-Cheatham, S.M., Gustin, M.S., Edwards, G.C., 2019. Evaluation of cation exchange membrane performance under exposure to high Hg0 and HgBr2 concentrations. Atmos. Meas. Tech. 12, 1207–1217.

Mohiuddin, K., Strezov, V., Nelson, P.F., Stelcer, E., 2014. Characterisation of trace metals in atmospheric particles in the vicinity of iron and steelmaking industries in Australia. Atmos. Environ. 83, 72–79.

NPI, 2017. Australian National Pollutant Inventory. Australian Government.

Obrist, D., Tas, E., Peleg, M., Matveev, V., Fain, X., Asaf, D., et al., 2011. Bromine-induced oxidation of mercury in the mid-latitude atmosphere. Nat. Geosci. 4, 22–26.

Pierce, A.M., Gustin, M.S., 2017. Development of a particulate mass measurement system for quantification of ambient reactive mercury. Environmental Science & Technology 51, 436–445.

Schroeder, W.H., Anlauf, K.G., Barrie, L.A., Lu, J.Y., Steffen, A., Schneeberger, D.R., et al., 1998. Arctic springtime depletion of mercury. Nature 394, 331.

Slemr, F., Angot, H., Dommergue, A., Magand, O., Barret, M., Weigelt, A., et al., 2015. Comparison of Mercury Concentrations Measured at Several Sites in the Southern Hemisphere. vol 15.

Soerensen, A.L., Skov, H., Jacob, D.J., Soerensen, B.T., Johnson, M.S., 2010. Global concentrations of gaseous elemental mercury and reactive gaseous mercury in the marine boundary layer. Environmental Science & Technology 44, 7425–7430.

Sommar, J., Andersson, M.E., Jacobi, H.W., 2010. Circumpolar measurements of speciated mercury, ozone and carbon monoxide in the boundary layer of the Arctic Ocean. Atmos. Chem. Phys. 10, 5031–5045.

Sprovieri, F., Pirrone, N., Hedgecock, I.M., Landis, M.S., Stevens, R.K., 2002. Intensive atmospheric mercury measurements at Terra Nova Bay in Antarctica during November and December 2000. Journal of Geophysical Research: Atmospheres 107, ACH 20–1-ACH 20-8.

Sprovieri, F., Hedgecock, I., Pirrone, N., 2010. An investigation of the origins of reactive gaseous mercury in the Mediterranean marine boundary layer. Atmos. Chem. Phys. 10, 3985–3997.

Sprovieri, F., Pirrone, N., Bencardino, M., D'Amore, F., Carbone, F., Cinnirella, S., et al., 2016. Atmospheric mercury concentrations observed at ground-based monitoring sites globally distributed in the framework of the GMOS network. Atmos. Chem. Phys. 16, 11915–11935.

Steffen, A., Schroeder, W., Bottenheim, J., Narayan, J., Fuentes, J.D., 2002. Atmospheric mercury concentrations: measurements and profiles near snow and ice surfaces in the Canadian Arctic during alert 2000. Atmos. Environ. 36, 2653–2661.
Steffen, A., Douglas, T., Amyot, M., Ariya, P., Aspmo, K., Berg, T., et al., 2008. A synthesis of atmospheric mercury depletion event chemistry in the atmosphere and snow. Atmos. Chem. Phys. 8, 1445–1482.
Steffen, A., Bottenheim, J., Cole, A., Douglas, T.A., Ebinghaus, R., Friess, U., et al., 2013. Atmospheric mercury over sea ice during the OASIS-2009 campaign. Atmos. Chem. Phys. 13, 7007–7021.
Strode, S., Jaeglé, L., Selin Noelle, E., Jacob Daniel, J., Park Rokjin, J., Yantosca Robert, M., et al., 2007. Air-sea exchange in the global mercury cycle. Glob. Biogeochem. Cycles 21.
Talbot, R., Mao, H., Feddersen, D., Smith, M., Kim, S., Sive, B., et al., 2011. Comparison of particulate mercury measured with manual and automated methods. Atmosphere 2, 1–20.
Temme, C., Einax, J.W., Ebinghaus, R., Schroeder, W.H., 2003. Measurements of atmospheric mercury species at a coastal site in the Antarctic and over the South Atlantic Ocean during polar summer. Environmental Science & Technology 37, 22–31.
Timonen, H., Ambrose, J., Jaffe, D., 2013. Oxidation of elemental Hg in anthropogenic and marine airmasses. Atmos. Chem. Phys. 13, 2827–2836.
UNEP, 2013. Minamata Convention on Mercury.
UNEP. Global Review of Mercury Monitoring Networks, 2016. United Nations Environment Programme, Geneva, Switzerland. p. 48.
Wang, F., Saiz-Lopez, A., Mahajan, A., Martin, J., Armstrong, D., Lemes, M., et al., 2014. Enhanced production of oxidised mercury over the tropical Pacific Ocean: a key missing oxidation pathway. Atmos. Chem. Phys. 14, 1323–1335.
Weiss-Penzias, P., Jaffe, D.A., McClintick, A., Prestbo, E.M., Landis, M.S., 2003. Gaseous elemental mercury in the marine boundary layer: evidence for rapid removal in anthropogenic pollution. Environmental Science & Technology 37, 3755–3763.
Weiss-Penzias, P., Jaffe, D., Swartzendruber, P., Hafner, W., Chand, D., Prestbo, E., 2007. Quantifying Asian and biomass burning sources of mercury using the Hg/CO ratio in pollution plumes observed at the Mount Bachelor observatory. Atmos. Environ. 41, 4366–4379.
Weiss-Penzias, P., Amos, H., Selin, N., Gustin, M., Jaffe, D., Obrist, D., et al., 2015. Use of a global model to understand speciated atmospheric mercury observations at five high-elevation sites. Atmos. Chem. Phys. 15, 1161–1173.
Wright, G., Gustin, M.S., Weiss-Penzias, P., Miller, M.B., 2014. Investigation of mercury deposition and potential sources at six sites from the Pacific Coast to the Great Basin, USA. Sci. Total Environ. 470-471, 1099–1113.
Zhang, L., Lyman, S., Mao, H., Lin, C., Gay, D., Wang, S., et al., 2017. A synthesis of research needs for improving the understanding of atmospheric mercury cycling. Atmos. Chem. Phys. 17, 9133–9144.